18th International Conference on Structural Mechanics in Reactor Technology (SMiRT 18)
Beijing, China, August 7-12, 2005
SMiRT18-O04-6

PROGRESS IN THE RELIABLE INSPECTION OF CAST STAINLESS STEEL REACTOR PIPING COMPONENTS

***SR Doctor**
Pacific Northwest National Laboratory
PO Box 999, Richland, WA. 99352 USA
Phone: 1-509-375-2495
Fax: 1-509-375-6497
E-mail: steven.doctor@pnl.gov

MT Anderson
Pacific Northwest National Laboratory
PO Box 999, Richland, WA. 99352 USA
Phone: 1-509-375-2523
Fax: 1-509-375-6497
E-mail: mike.anderson@pnl.gov

AA Diaz
Pacific Northwest National Laboratory
PO Box 999, Richland, WA. 99352 USA
Phone: 1-509-375-2606, Fax: 1-509-375-6497
E-mail: aaron.diaz@pnl.gov

SE Cumblidge
Pacific Northwest National Laboratory
PO Box 999, Richland, WA. 99352 USA
Phone: 1-509-372-4054, Fax: 1-509-375-6497
E-mail: stephen.cumblidge@pnl.gov

ABSTRACT

Studies conducted at the Pacific Northwest National Laboratory (PNNL) in Richland, Washington, have focused on assessing the effectiveness and reliability of novel NDE approaches for the inspection of coarse-grained, cast stainless steel reactor components. The primary objective of this work is to provide information to the United States Nuclear Regulatory Commission (US NRC) on the utility, effectiveness and reliability of ultrasonic testing (UT) and eddy current testing (ET) inspection techniques as related to the inservice ultrasonic inspection of primary piping components in pressurized water reactors (PWRs). This paper describes progress, recent developments and results from assessments of three different NDE approaches including ultrasonic phased array inspection techniques, eddy current testing for surface-breaking flaws, and a low-frequency ultrasonic inspection methodology coupled with a synthetic aperture focusing technique (SAFT). Westinghouse Owner's Group (WOG) cast stainless steel pipe segments with thermal and mechanical fatigue cracks, PNNL samples containing thermal fatigue cracks and several blank spool pieces were used for assessing the inspection methods. Eddy current studies were conducted on the inner diameter (ID) surface of piping specimens while the ultrasonic inspection methods were applied from the outer diameter (OD) surface of the specimens. The eddy current technique employed a Zetec MIZ-27SI Eddy Current instrument and a Zetec Z0000857-1 cross point spot probe with an operating frequency of 250 kHz. In order to reduce noise effects, degaussing of a subset of the samples resulted in noticeable improvements. The phased array approach was implemented using an R/D Tech Tomoscan III system operating at 1 MHz, providing composite volumetric images of the samples. The low-frequency ultrasonic method employs a zone-focused, multi-incident angle inspection protocol (operating at 250-500 kHz) coupled with SAFT for improved signal-to-noise and advanced imaging capabilities. A variety of dual-element, custom designed low-frequency probes (fixed-wedge and variable angle configurations) were employed in laboratory trials. Results from laboratory studies for assessing detection, localization and length sizing effectiveness are discussed. This work was sponsored by the U.S. Nuclear Regulatory Commission under Contract DE-AC06-76RLO 1830; NRC JCN Y6604; Mr. Wallace Norris, Program Monitor.

Keywords: ultrasonic, phased array, eddy current, SAFT, cast stainless steel.

1. INTRODUCTION

The relatively low cost and corrosion resistance of cast stainless steel (CSS) have resulted in extensive use of this material in the primary piping systems of Westinghouse-designed PWRs. Inservice inspection requirements dictate that piping welds in the primary pressure boundary of light water reactors (LWRs) be subject to a volumetric examination based on the requirements of Section XI of the ASME Boiler and Pressure Vessel Code. The volumetric examination may be either radiographic or ultrasonic. For inservice examinations, background radiation and access limitations generally prevent the use of radiography. Hence, cast austenitic welds in primary piping loops of LWRs are subject to ultrasonic inservice inspection. The purpose of ultrasonic inservice inspection of nuclear reactor piping and pressure vessels is the reliable detection and accurate sizing of material defects. Before defects can be sized, they must first be detected. Detection is accomplished by analyzing ultrasonic echo waveforms from material defects. Due to the coarse microstructure of CSS material, many inspection problems exist and are common to structures such as statically cast elbows, statically cast pump bowls, centrifugally cast stainless steel (CCSS) piping, dissimilar metal welds, and weld-overlay-repaired pipe joints. Far-side weld inspection of stainless steels is an inspection technique included in the work scope since the ultrasonic field must pass through weld material.

Because Westinghouse Electric Corporation manufactured and implemented CCSS piping in the primary reactor coolant loop network of 27 PWRs in the U.S., there exists a need to develop effective and reliable inspection techniques for these components. Examination of CCSS materials is difficult to perform due to the coarse microstructure that characterizes these materials. The general microstructural classifications for CCSS are columnar, equiaxed, and a mixed columnar-equiaxed condition of which the majority of field material is believed to be the latter.

CCSS is an anisotropic and inhomogeneous material. The manufacturing process can result in the formation of a long columnar grain structure, (approximately normal to the surface) with grain growth oriented along the direction of heat dissipation, often several centimeters in length. During the solidification of the material, columnar, equiaxed (randomly speckled microstructure), or a mixed structure can result depending on chemical content and control of the cooling process.

The large size of the anisotropic grains, relative to the acoustic pulse wavelength, strongly affects the propagation of ultrasound by causing severe attenuation, changes in velocity, and scattering of ultrasonic energy. Refraction and reflection of the sound beam occur at the grain boundaries resulting in defects being incorrectly reported, specific volumes of material not being examined, or both. When coherent reflection and scattering of the sound beam occur at grain boundaries, ultrasonic indications occur which are difficult to distinguish from signals originating from flaws. When inspecting pipe sections where the signal-to-noise ratio is relatively low, ultrasonic examinations can be confusing, unpredictable, and unreliable (Taylor, 1984).

2. OBJECTIVE OF THE STUDY

The objective of this research is to determine the effectiveness and reliability of ultrasonic inspection techniques on LWR components containing cast stainless steel material and other coarse-grained components with dissimilar metal welds, piping with corrosion-resistant cladding, and far-side examinations of austenitic piping welds. In particular, to evaluate and enhance various NDE methods to directly improve our ability to discriminate between coherent ultrasonic energy scattered from grain boundaries (geometric reflectors) and cracks (discontinuities, etc.) in coarse grained steel components.

Throughout many industrial sectors, efforts are underway to evaluate the potential for new nondestructive examination (NDE) methods to reliably detect structural degradation in aging components while controlling costs and limiting inspection times. In particular, the nuclear industry, through the Electric Power Research Institute (EPRI), is actively involved in determining the feasibility of applying new NDE methods for particularly challenging inspections at operating nuclear power plants. This report provides a synopsis of the results of laboratory investigations at PNNL to determine capabilities of ultrasonic phased array (PA), low-frequency/SAFT, and eddy current testing (ET) as applied to the inspection of cast stainless steel welds in nuclear reactor piping.

PNNL chose to evaluate three advanced technical approaches in this study. The phased array approach was selected because industry is evaluating this state-of-the-art technology for several applications and anecdotal information indicates that there appear to be “windows” where effective inspections can be made through coarse grained microstructures. It is not known if these “windows” are related to inspection frequency, inspection angle, or some other microstructural feature. The use of the

phased array technology provides the capability to assess the effect of inspection angles. The low-frequency/SAFT approach was chosen because of its previous success in cast stainless steel round robin trials, laboratory testing, and the fact that the use of lower frequencies corresponds to longer wavelengths which are typically larger than the average grain diameter exhibited by CSS microstructures, effectively reducing the impact of the microstructure on the sound field (Diaz, et al., 1998). This technique employs a protocol that allows for the composite evaluation of multiple inspection angles, modalities and frequencies, as well as both near- and far-side inspection orientations. PNNL had tracked the success of an inside-surface, inner diameter (ID) eddy current test that had been employed at VC Summer in 2000 on primary piping nozzle to pipe welds. At VC Summer there were some challenging ID geometry conditions that adversely impacted the ultrasonic testing, but were easily handled by the small footprint of the eddy current probe. The eddy current inspection results were validated by destructive testing with all indications being confirmed to be cracks, with the exception of one indication that was caused by an iron rich subsurface inclusion (Rao et al. 2001). PNNL employed a similar eddy current method for this study.

3. BACKGROUND OF NDE APPROACHES EVALUATED IN THE STUDY

3.1 Low-frequency/SAFT-UT approach

The low-frequency/SAFT-UT inspection technique uses a zone-focused, high-bandwidth, low frequency (250 kHz to 450 kHz) inspection protocol coupled with the synthetic aperture focusing technique, referred to as "SAFT" (Hall, et al. 1988; Doctor et al. 1996). The examination protocol is based upon the premise that there exist sufficient differences between the characteristics of coherently scattered ultrasonic energy from grain boundaries and geometrical reflectors, and the scattered ultrasonic energy from surface breaking fatigue and stress corrosion cracks in wrought austenitic piping welds. PNNL's empirical approach relies on the strategy that acoustic impedance variations at the grain boundaries (and in the heat affected zone along the weld fusion lines), can be minimized by using lower frequencies (longer wavelengths), and the degree of coherent energy scattered from these boundaries should be inconsistent as a function of frequency, insonification angle, scan direction, and the amplitude of returning signals. The low frequency-SAFT approach is directed toward detecting the corner-trap response from the surface breaking crack as a function of time and spatial position. If the frequency is low enough, the examination is less sensitive to geometry and the effects of the microstructure and the probability of detection should increase for surface breaking cracks. The tradeoff is resolution. However, with the addition of SAFT signal processing, the examination can be performed at lower frequencies while maintaining the capability to suitably size the detected cracks. Therefore, by utilizing multiple examination frequencies and incident angles, and inspecting from both sides of a weld, the low frequency SAFT technique invokes a composite approach for detection, localization and sizing of cracks in these types of materials.

The examination process is further enhanced by the addition of a low frequency, variable angle, high bandwidth search unit which enables the inspector to compensate for acoustic velocity variations due to the microstructure by selecting the optimal incident angle in the material under test. The high bandwidth allows the inspector to utilize a wide range of examination frequencies centered near 350 kHz. This effectively provides a single transducer platform for obtaining multiple angle scans over a frequency range from 250 kHz to 450 kHz. The zone-focal characteristics of the dual element search unit provide optimal insonification of the inner surface (ID) over a range of incident angles for pipe wall thicknesses. The plano-concave shape of the transmitting crystal element helps to establish the search unit's bandwidth and improve its zone focusing characteristics. The design allows for variable-angle inspections (0° to 70° RL) without the need to mount the elements on different sets of angled wedges (shoes). The two crystal elements are mounted into a small cylinder at a roof angle of 4.07° from the normal, and the unit is designed with a zone focus (approximately 6.35 cm to 10.16 cm deep in CSS material). For the variable angle transducer calibration, the end of block geometry was used as a target indicator for identification and selection of the proper incident angle in the material under test. Specimen thicknesses were measured, surface contour sketches were drawn, and inner surface dimensional data were recorded and used in portions of the data analysis.

Since the inspection technique takes advantage of multiple frequencies and both longitudinal and shear wave-modes, the wavelength (and effectively the resolution capability) will vary as a function of frequency and wave-mode. The longitudinal-wave acoustic velocity in 304 stainless steel material is 5.790 mm/μs, while the shear-wave acoustic velocity is 3.180 mm/μs. For 250 kHz L-wave inspections, the wavelength is 2.32 cm, and for shear-wave inspections the wavelength is 1.27 cm. For 400 kHz L-wave inspections, the wavelength is 1.45 cm, and for shear-wave inspections the wavelength is 0.79

cm.

The final segment of this process utilizes an advanced synthetic aperture focusing technique known as SAFT. "Synthetic aperture focusing" refers to a process in which the focal properties of a large-aperture focused transducer are synthetically generated from data collected over a large area using a small transducer with a divergent sound field. The processing required to focus this collection of data has been called beam-forming, coherent summation, or synthetic aperture processing. The resultant image is a full-volume focused characterization of the inspected area (Doctor, et al, 1996).

SAFT technology is able to provide significant enhancements to the inspection of austenitic welds and other anisotropic, coarse grained materials. The resolution of an imaging system is limited by the effective aperture area; that is, the area over which data can be generated, collected, and processed. SAFT is an imaging method which was developed to overcome some of the limitations imposed by large physical apertures, and has been successfully applied in the field of ultrasonic testing. Relying on the physics of ultrasonic wave propagation, SAFT is a very robust technique. Utilizing a pitch-catch configuration for typical data collection throughout these activities, the transducer was positioned on the surface of the specimens, and RF ultrasonic data were collected. As the transducer was scanned over the surface of the specimens, the A-scan radio frequency (RF) waveform was amplified, filtered, and digitized for each position of the transducer. An A-scan is simply an electronic presentation of reflected energy displayed as amplitude versus time. Each introduced flaw produced a collection of echoes in the A-scan records. The unprocessed or RF data sets were then post-processed using the SAFT algorithm, invoking a variety of full beam angle values (between 6º and 24º) in order to evaluate and optimize the temporal/spatial averaging enhancement.

If the reflector is an elementary single point reflector, then the collection of echoes will form a hyperbolic surface within the data-set volume. The shape of the hyperboloid is determined by the depth of the flaws in the specimens and the velocity of sound in the specimens. This relationship between echo location in the series of A-scans and the actual location of the introduced flaws within the specimen makes it possible to reconstruct a high-resolution, high signal-to-noise ratio image from the acquired raw data. If the scanning and surface geometries are well known, it is possible to accurately predict the shape of the locus of echoes for each point within the test object. The process of coherent summation for each image point involves shifting a locus of A-scans, within a regional aperture, by predicted time delays and summing the shifted A-scans. This process may also be viewed as performing a temporal/spatial matched filter operation for each point within the volume to be imaged (Hall, et al., 1988).

Each element is then averaged by the number of points that were summed to produce the final processed value. If the particular location correlates with the elementary point response hyperboloid, then the values summed will be in phase and produce a high-amplitude result. If the location does not correlate with the predicted response, then destructive interference will take place and the spatial average will result in a low amplitude value; thus, reducing the noise level to a very small value. SAFT processing is also effective at removing constant-time signals that are not near the front surface, and sub-volume selection during data analysis readily removes any residual near-surface signals.

3.2 Phased array approach

Recent advances in electronics miniaturization, computer processing capabilities, and fabrication methods for ultrasonic transducers have enabled phased array technology to become a viable approach for many field applications. The geometrical design of a PA transducer is typically a function of specific implementation variables, i.e., geometries such as linear, annular, circular, or matrix designs are developed to address a particular ultrasonic application need (Poguet, et al., 2001). However, the basic premise for all PA transducers involves a set of small, individual piezoelectric elements that are independently driven. Although these elements may be pulsed individually, or in groups, to simulate conventional transducer excitation, the real strength of this technique lies in the capability of the system to electronically delay each of these elements during both generation and reception of ultrasonic sound fields. The wave-fronts produced by subsets of elements interfere within the inspected component to produce a resultant, phase-integrated ultrasonic wave. This is commonly referred to as beam forming. The PA system can therefore steer and focus the integrated ultrasonic beam within the component.

Generally, all PA ultrasonic systems are computer-controlled enabling software to define the groups and sequences of elements being electronically delayed. Parameters such as the number of individual elements in a virtual element, the delay sequence for firing of the virtual elements, element amplitudes, and the delays in reception, are programmed into the system operating software. The setting of these generation and reception parameters for a particular response is called a focal law.

Since practically all aspects of the sound beam are being controlled electronically, many iterations, or sequences of iterations, can be run in nearly real time. This allows a single array to inspect a component with variable inspection angles and focusing depths almost simultaneously. For instance, depending on the array design and the component thickness, a one-dimensional linear array, with major axis oriented normal to a pipe weld, may interrogate close to an entire planar cross-section of the weld by sweeping through a series of inspection angles without having to mechanically move the transducer toward and away from the weld. Theoretically, an entire pipe weld can then be examined with a single circumferential scan motion. Most PA systems capture, digitize and store the ultrasonic data, which enhances repeatability and permits off-line analysis and imaging. Specialized computer software and hardware (including upgraded virtual and hard disc memory) are needed to support analyses of PA data. Also, because of the variations of images that can be produced, a systematic method should be employed when performing these analyses by using a standardized procedure (Anderson, et al., 2003).

The phased array system at PNNL consists of a Tomoscan III® 32 channel instrument, produced off-the-shelf by ZETEC (formerly R/D Tech, Inc.). This is a standard piece of equipment used for PA applications in several industrial sectors. This type of system is used by General Electric to inspect reactor internals and at the EPRI NDE Center for a variety of applications including far-side inspection procedure development and initial "true state" characterization of Performance Demonstration Initiative (PDI) specimens. The instrument can be programmed (by development of focal laws) to control up to 32 channels for transmission and reception of ultrasonic signals. It has 12-bit logic and operates through a local ethernet connection to a standard desktop computer.

3.3 Eddy current testing approach

Eddy current testing can be used for a variety of applications such as the detection of cracks, measurement of metal thickness, detection of metal thinning due to corrosion and erosion, determination of coating thickness, and the measurement of electrical conductivity and magnetic permeability. Eddy current inspection is an excellent method for detecting surface and near surface defects. Defects such as cracks are detected when they disrupt the path of the eddy current field.

Factors such as the type of material, surface finish and condition of the material, the design of the probe, and many other factors can affect the sensitivity of the inspection. Eddy current data were collected using an automated scanning system to improve the quality of the measurements and to construct images of the scanned areas. Typically, the most common type of scanning is line scanning where an automated system is used to push the probe at a fixed speed. Two-dimensional scanning systems are used to scan a two-dimensional area. This is typically embodied in a scanning system that scans in an X-Y raster mode. The data is then displayed as a false-color plot of signal strength or phase angle shift as a function of position, similar to an ultrasonic C-scan presentation.

Automated scanning advantages when using eddy current testing methods, include:

- Minimizes changes in liftoff or fill factor resulting from probe wobble, uneven surfaces, and eccentricity of tubes.
- Accurate indexing.
- Repeatability.
- High resolution mapping.

The CSS examinations were implemented using a PC-controlled X-Y scanning system connected to a ZETEC MIZ27-SI eddy current. A ZETEC plus (+) point probe configured with 2 small coils set 90 degrees apart from each other was chosen. The probe was fitted to a spring-loaded probe sled which had the ability to pivot and gimbal to ensure adequate contact of the probe face to the sample surface throughout the scanning operation. A calibration block was used to set the instrument parameters (liftoff, probe drive and gain) and scanner parameters (speed and spacing between scans) to achieve the best signal response. Three frequencies were evaluated including, 100 kHz, 250 kHz, and 500 kHz. The frequency of 250 kHz resulted in the best overall response for small surface defects and provided lower noise resulting in a higher signal to noise ratio for the detected indications.

The scan area was defined as 6.35 cm on each side and parallel to the center line of the weld and 2.54 cm from the top and bottom edges of the test sample, to minimize the edge effects on the probe which could suppress signals from defects near the edge of the scan area. Valid flaw indications resulting from planar crack-like defects had a typical phase response ranging between 65º and 105º or 245º and 285º and a length greater than 0.64 cm. Indicated flaws were checked and then subsequently re-scanned to validate flaw detection. The lengths and locations of the flaws were determined using the

data collection and analysis software.

Those samples that exhibited high noise levels in the scan area were degaussed then re-scanned with favorable results obtained on one half of the samples. Areas where results were difficult to interpret, or were otherwise suspicious, were also re-scanned and categorized as "hot spots". These discontinuities were generally in the range between 0.64 cm and 1.27 cm in length.

4. CSS SPECIMENS USED IN THIS STUDY

This study focused on examination of Westinghouse Owner's Group (WOG) CSS specimens, PNNL samples, and several blank spool pieces. These specimens represent a variety of reactor piping configurations including:

- Statically cast elbow to centrifugally cast pipe.
- Carbon steel inlet nozzle to forged SS safe-end to statically cast elbow.
- Statically cast pump outlet nozzle to centrifugally cast pipe.

The represented microstructures were described as "coarse" and "coarse-mixed" microstructures, consisting of combined dendritic (columnar) and equiaxed grains. The photograph in Figure 1 shows the WOG sample specimens co-located in the Laboratory prior to data acquisition.

The cracks in the WOG pipe sections were created using methods that have proven useful in producing realistic surface-connected mechanical and thermal fatigue cracks. The flaws in the WOG specimens are basically considered to be planar cracks, parallel to the weld centerline, and perpendicular to and connected to the inner diameter. However, the fabrication process has also created some transverse cracking in some of these specimens. The tightness and roughness of the thermal fatigue cracks generally make them more difficult to detect in comparison to mechanical fatigue cracks.

Fig. 1. Westinghouse Owner's Group sample set of CSS specimens used in this study.

5. EXAMINATION RESULTS

5.1 Low-frequency/SAFT-UT results from the outer pipe surface

The data analysis protocol must address multiple data sets for crack identification, localization and sizing. The analysis technique is time-intensive and is based upon redundancy of the ultrasonic indications as a function of the various inspection parameters. Scans were performed at various angles and frequencies and, when possible, from both sides of the weld. Each scan was separately analyzed for indications and the data is then combined. The plots were examined visually to determine what indications appeared to recur most often, which (if any) were geometrical features, and which seemed to

be grain noise or other irrelevant indications. The most likely cluster was used to determine the crack location. In some cases an arithmetic average of the endpoints was used; in other cases, a visual estimate was used; this has the advantage of allowing the inspector to assign (implicit) weights to the data sets.

In the work leading up to this study, it had been determined that by employing wavelengths longer than the average grain diameter of the microstructure, the low frequency/SAFT inspection system could consistently detect geometrical reflectors, notches (25% deep), sawcuts (25% deep), side-drilled holes (1/8 T) and fatigue-type cracking in thinner-walled CSS materials that were at least 30% through-wall in depth and greater, and with a minimal extent of 2.54 cm. (1.0 in.) or longer. The system detection limits for ID connected fatigue cracks have been determined to be approximately 30% through-wall and greater. If a crack is shallower than 30% of the part thickness, assuming CSS material structure with thicknesses between 5.6 cm. and 8.9 cm., the low frequency-SAFT inspection system will probably not detect it. Therefore, throughout this study, these examinations were conducted at the lower limits of detection for the low frequency-SAFT technique. Ten of the WOG specimens (see Table 1) with the largest flaw dimensions were identified as the focus of the low-frequency/SAFT portion of the study.

Of the ten WOG specimens listed in Table 1, the four specimens in Table 2 contained the largest flaw dimensions in the entire set. The first phase of the study employed commercially procured, custom designed variable angle and fixed-wedge transducers operating over a frequency range from 250 to 450 kHz. The analysis showed that the LF-SAFT technique can utilize both longitudinal-wave (L-L) signal responses and mode converted longitudinal to shear (L-S) wave signal responses as well. Reflected signals from flaws were often detected using both L-L and L-S signal

Table 1 WOG Specimen Flaw Information.

Specimen ID	Actual Flaw Depth (% Through Wall)	Actual Flaw Length	Location of Flaw (Side of Weld)	Type of Crack (Mechanical or Thermal Fatigue)
1	1.1 cm (15.7% TW)	3.94 cm	Elbow	MF
2	1.27 cm (17.9% TW)	4.19 cm	Pipe	MF
3	2.64 cm (40.8% TW)	6.99 cm	Elbow	MF
4	1.85 cm (29.2% TW)	6.86 cm	Elbow	TF
5	2.54 cm (40.0% TW)	6.73 cm	Pipe	MF
6	1.5 cm (23.6% TW)	5.92 cm	Elbow	TF
7	1.27 cm (23.3% TW)	4.19 cm	Elbow	MF
8	1.63 cm (29.8% TW)	6.15 cm	Elbow	TF
9	2.55 cm (34.2% TW)	6.78 cm	Elbow	MF
10	1.5 cm (20.0% TW)	5.72 cm	Pipe	TF

Table 2 depicts those flaws where multiple detections resulted in a composite measurement of the flaw position and length.

Table 2 Actual versus measured values for detection results of the four WOG specimens containing the largest flaws.

WOG ID	Actual Flaw Depth (% Through-wall)	Actual Flaw Length	Measured Length -6dB	Signal-to-Noise Ratio (dB)
3	2.64 cm (40.8% TW)	6.99 cm	7.37 cm	5.4 dB
5	2.54 cm (40.0% TW)	6.73 cm	7.11 cm	6.1 dB
8	1.63 cm (29.8% TW)	6.15 cm	5.46 cm	5.6 dB
9	2.55 cm (34.2% TW)	6.78 cm	5.89 cm	6.6 dB

returns, thus lending yet another confirmatory method for validating the discrimination between flaws and microstructural effects. It should be noted that analysis of the inlet nozzle to safe-end to elbow specimens only used data acquired from the statically cast elbow side of the weld. Data was not acquired on the forged stainless steel side of the weld. An example of the LF-SAFT data is shown in Figure 2.

Results from data acquired with these transducers indicated that the smaller flaws were not detected. Only those flaws in Table 2 were detected, localized and subsequently length sized.

A third trial was conducted to acquire low-frequency ultrasonic data on this same set of CSS specimens in order to assess the detection performance of an additional custom probe that was loaned to PNNL for a brief period of time. The data was taken using a low-frequency, broadband (500 kHz) transmit-receive longitudinal (TRL) probe on loan from AIB Vincotte. The broadband 45-degree probe was excited using a tunable square-wave input pulse with pulse durations corresponding to three frequencies, 300 kHz, 415 kHz, and 500 kHz, to examine the influence of the examination frequency on the detectability of the cracks in the WOG samples. The transducer had a nominal center frequency and peak operating frequency at approximately 500 kHz. Both transmit and receive elements of the transducer were fabricated from monolithic rectangular crystals (with dimensions 25.4 mm x 38.1 mm), in a fixed housing. The transducer was configured for a 45º incident angle in the material using the longitudinal-wave inspection modality. The surface contacting wear-face of the transducer was gently sanded to more effectively fit the contour of the WOG specimen surface curvature, essentially eliminating any rocking and providing suitable coupling to the surface. An example of the SAFT processed ultrasonic data from this set of scans is illustrated in Figure 3.

Specimen 9: Pump Outlet Nozzle to Pipe Configuration SCSS-CCSS

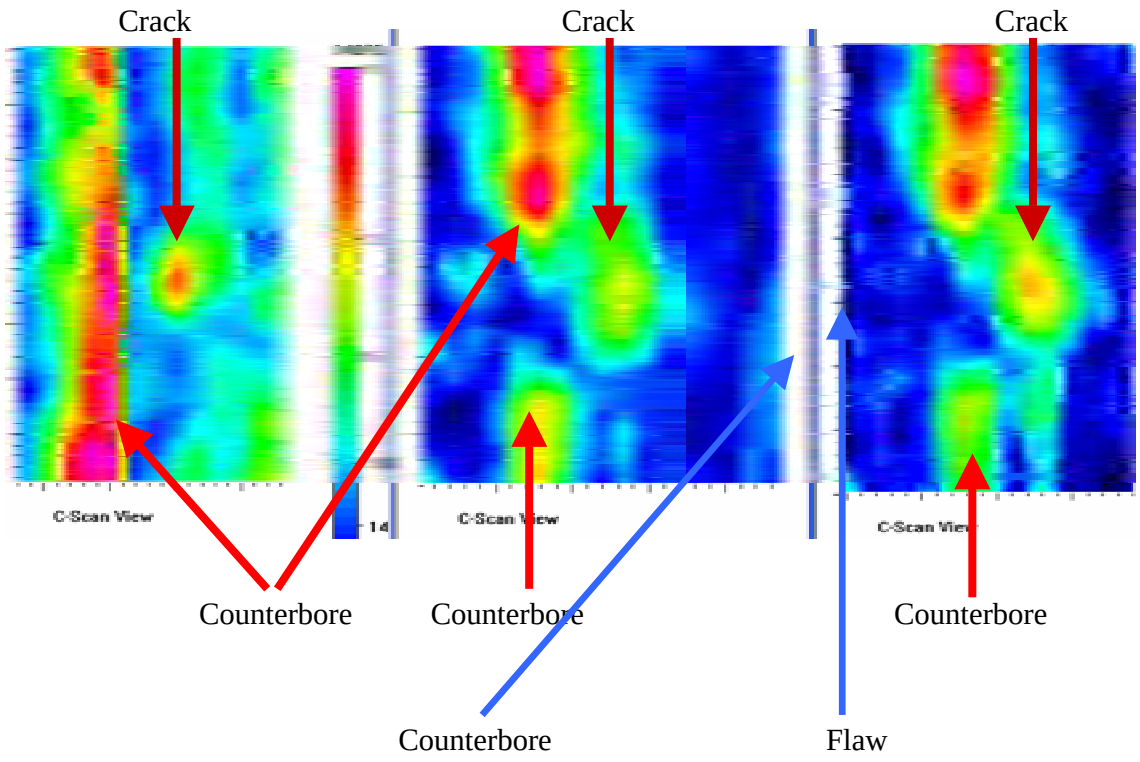

Fig. 2. C-Scan view left: 400 kHz, 45 deg. from the elbow (SCSS) side of the specimen. 24 deg. SAFT Beam processing angle. C-Scan View Mid: 350 kHz, 30 deg. From the pipe (CCSS) side of the specimen. 24 deg. SAFT beam processing angle. C-Scan view right: 250 kHz, 30 deg. From the pipe (CCSS) side of the specimen. 24 deg. SAFT beam processing Angle.

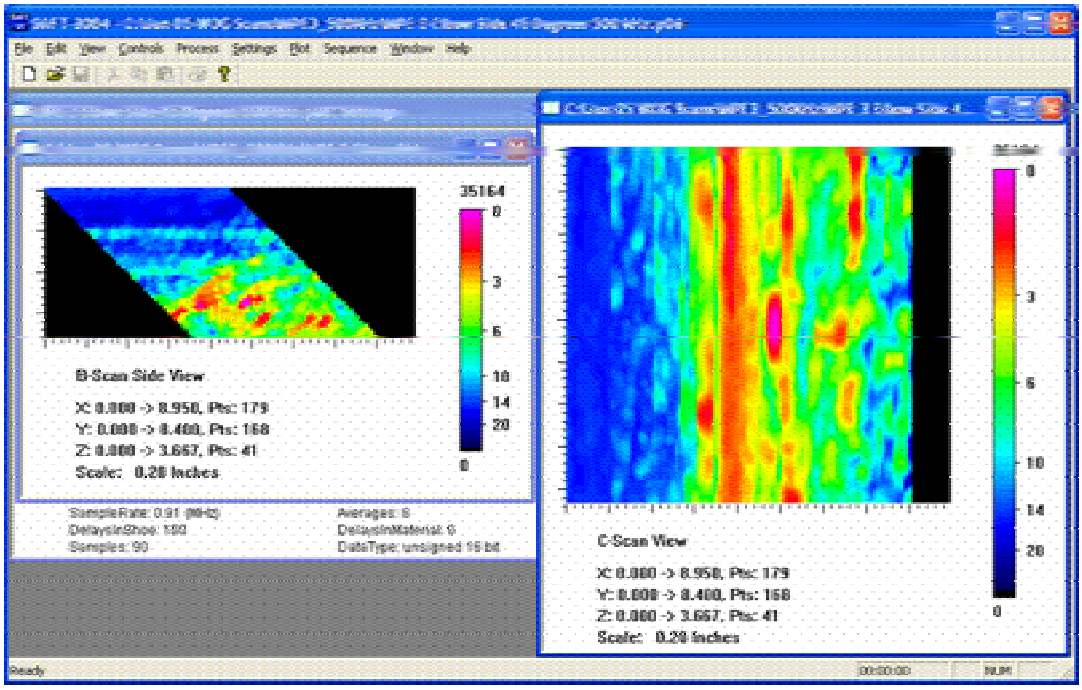

Fig. 3. Composite B-scan (side-view) and C-scan (top-view) views of SAFT processed images resulting from a 500 kHz, 45 degree, L-wave scan of WOG specimen 5.

The results from scans of WOG specimen 5 exhibited a higher amount of scattered energy from the microstructure than that found with the other transducers. As expected, the higher operational and center frequency (500 kHz) of the probe resulted in an increase in sound field attenuation and higher levels of coherently scattered energy from grain boundaries within the material. The resultant analysis from data acquired on WOG samples 5, 8 and 10, showed that only the largest flaw (in WOG specimen 5) was detected.

5.2 Phased array results from the outer pipe surface

One of the advantages of phased array (PA) data is that all information is stored digitally during each scan, allowing off-line processing and interpretation to be performed in an environment better suited for analysis than one usually encounters during data acquisition. Several image channels of the data can be displayed, based on the preference of the analyst. The volume corrected B-, C- and S-scan images, along with supplemental A-scans, were used to assist our understanding of the data. For the TomoView® PA software used during these trials, the B-scan image is a projection of the sound field through the component, oriented as if looking along the direction of sound propagation, displaying a circumferential cross-section of the weld. The sector view (S-scan) provides a projection of the sound fields (from initial to final angle being used, i.e., 30° to 60° for the TRL array). C-scan images are X-Y planar projections of the sound field, and A-scan representations illustrate the electronic time-based waveform responses for reflectors based time and amplitude, respectively. Each of the B and S-scan images contain all data in the linear scan. Measurement, gating and sound field cursors are used to provide “slices” of material to view along the projected sound beam and discrete beam angle responses are shown in the A-scan representation. By manipulating a set of cursors, the analyst is able to “walk-through” cross-sections of the material along each linear scan. One important analysis tool of the phased array system is the ability to examine each angle individually. This allows the investigator to view the different response images in a given scan and discriminate between the various features in a

specimen.

This work was performed using a 1 MHz phased-array probe. The probe was raster-scanned over the welds while sweeping from 30-60 degrees in 3-degree steps. This combination of raster scanning and angle sweeping allows for the collection of massive amounts of data on the samples very quickly. Figures 4 and 5 illustrate PA data images from a pipe-to-elbow configuration.

From an analysis of the PA data, two out of twelve cracks were detectable through centrifugally cast material, resulting in 17% of all cracks examined using this inspection method. Eight of eleven cracks were detectable through statically cast material, resulting in 72% of all cracks examined. Due to beam re-direction and attenuation at 1.0 MHz, flaws could not consistently be distinguished from geometry. Depth-sizing of the cracks was not possible in any specimen as crack tip signals were not detected.

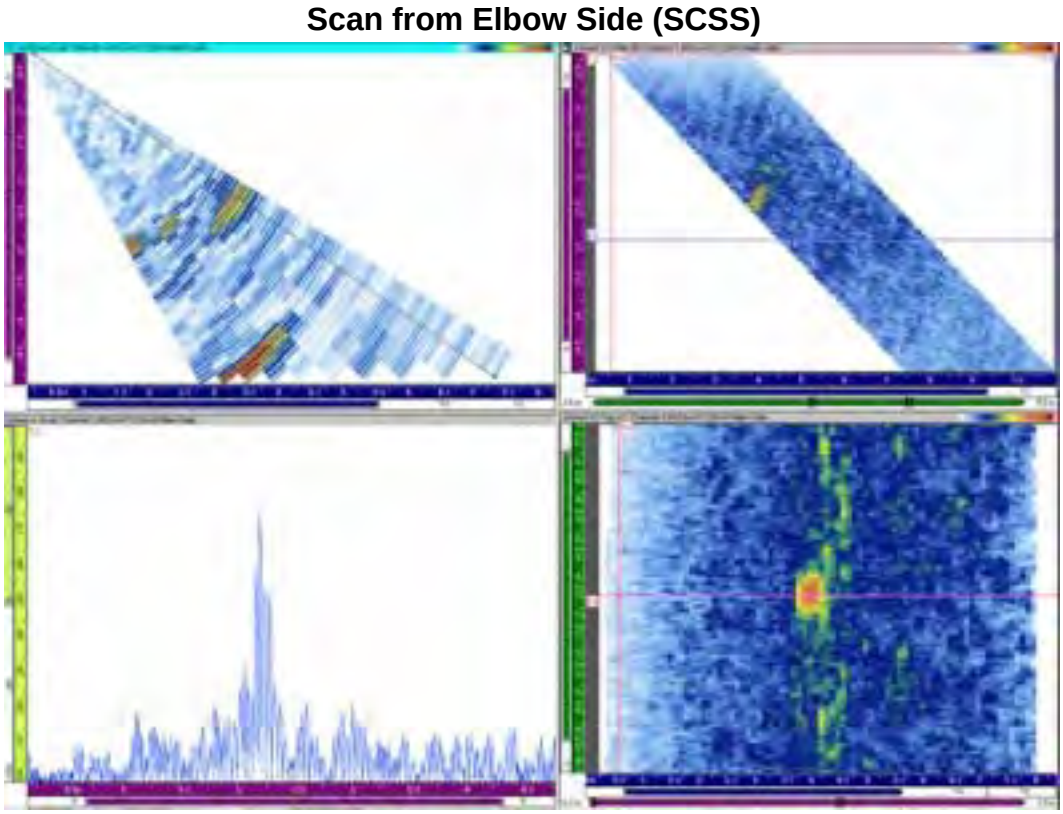

Fig. 4. PA image illustrating a flaw in a pipe-to-elbow weld imaged using a 1 MHz phased array probe from the statically cast (SCSS), elbow side of the weld. The crack is located on the elbow side of the weld.

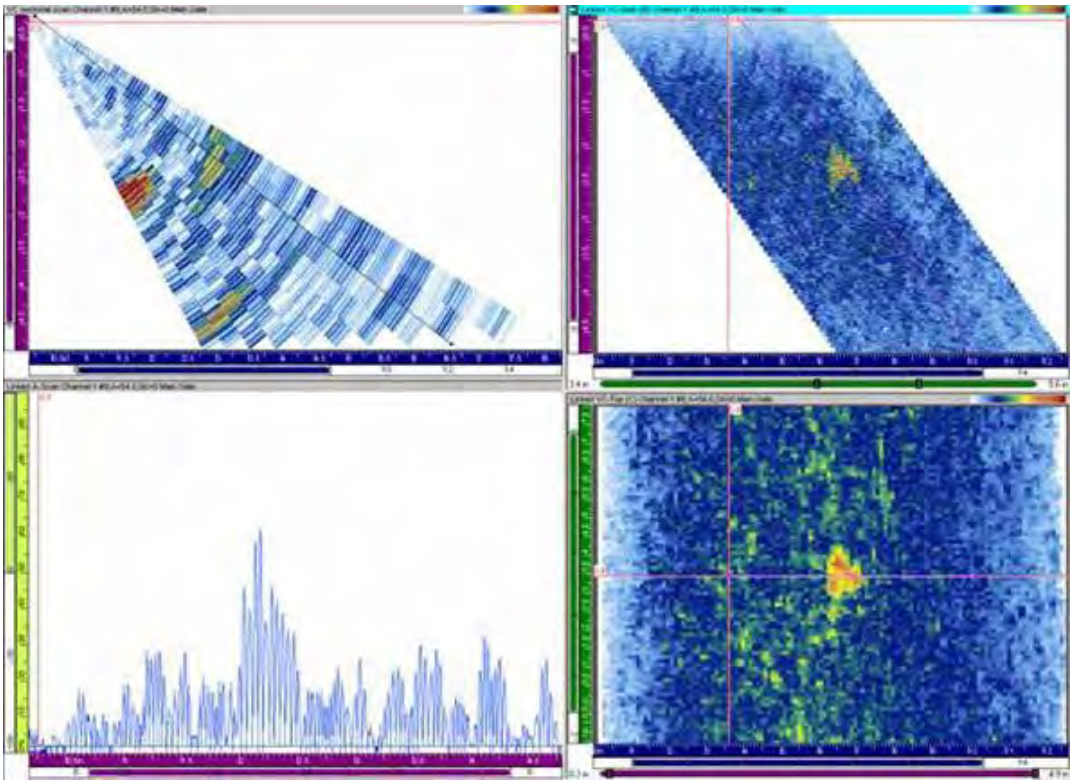

Fig. 5. PA image illustrating the same flaw in figure 4, imaged using a 1 MHz phased array probe from the centrifugally cast (CCSS), pipe side of the weld. The crack is located on the elbow side of the weld.

5.3 Eddy current results from the inner pipe surface

Using ID surface, eddy current testing techniques magnitude and phase plots were generated to visualize the data. An example of the imaged eddy current data is shown in Figure 6.

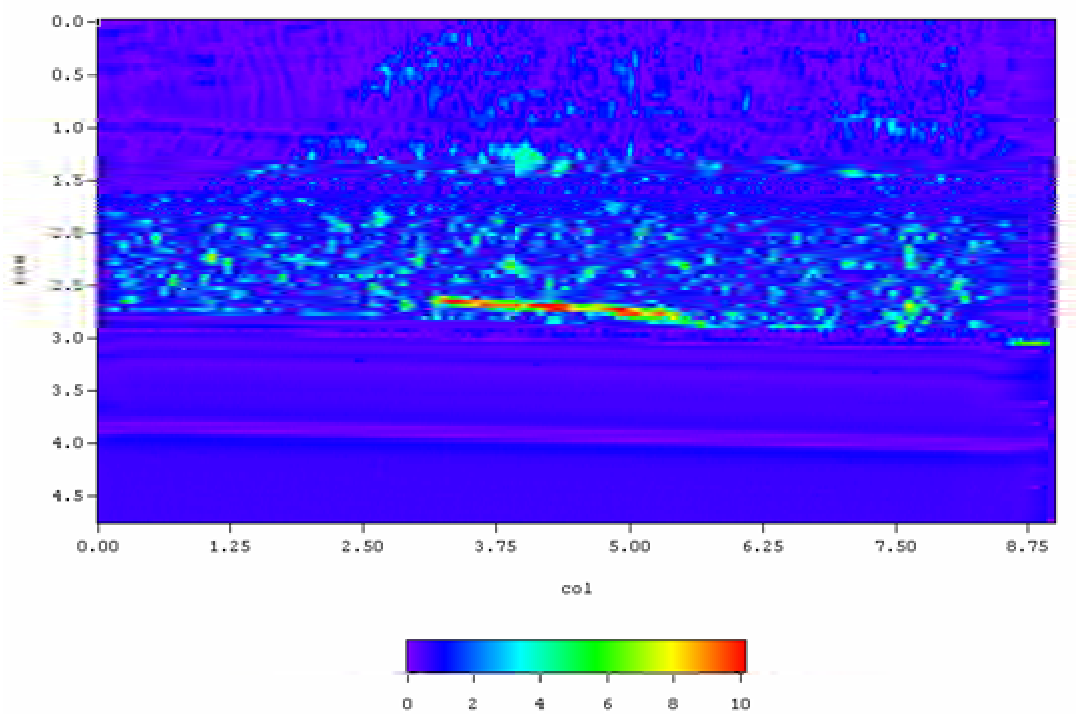

Fig. 6. De-gaussed magnitude plot of WOG specimen number 3 at 250 kHz.

For analysis of the ET data, loss of signal was used for length sizing the indications. From this analysis, 16 of 19 of the detected flaws in the study were undersized, and the associated length RMSE was 9.3 mm. Noise signals that would be confused with crack signals having high amplitude and correct phase were also evident in the data. From this set of anomalous indications, eleven detection scenarios resulted in miss-called cracks with an average length of 9.4 mm over a range of lengths from 3.1 to 19.5 mm. ET was very effective in that all of the cracks were detected, and both magnitude and phase angle images were useful in detecting the cracks. Demagnetizing the inspection zones proved useful 50% of the time.

6. CONCLUSION

The results from assessing low-frequency ultrasound coupled with SAFT indicate that employing longer-wavelengths can indeed improve detection performance by providing an inspection sound field that is less sensitive to the effects of the cast microstructures. All the cracks greater than 30% of the wall thickness were detected with an appropriate probe design, using the LF-SAFT technique. The results indicate that the multi-frequency/angle/orientation approach is effective in detection of fatigue cracks in CSS where typical flaw depth is approximately 30% through-wall and flaw length is approximately 25 mm in extent or greater. By employing such long wavelengths, it is shown that detection performance for cracks with depths less than 30% is poor, in large part due to the lack of sensitivity to smaller reflectors. Finally, the crack detection criteria needs further validation against data acquired on uncracked specimens.

Inspection from the outside surface of the pipe is aided by advances in signal processing, and it is shown that state-of-the-art advances such as phased array methodologies can further improve detection performance as the inspection frequency is reduced. Lower frequency (350-450 kHz), high bandwidth arrays may be able to penetrate and focus energy through CCSS materials. The results here indicate that phased array technology should improve the state-of-the-art for crack detection in coarse-grained materials. For statically cast materials, the results are very good at 1.0 MHz, but lower frequency PA probes are needed to reliably inspect centrifugally cast microstructures effectively.

If the inner surface is accessible, the ET method demonstrated here is very effective for detection of these types of surface breaking cracks. It should be noted that none of the techniques evaluated in this study provided depth sizing information. Future additional testing is needed to further evaluate the three methods described here, on other field-representative coarse grained material specimens. Other studies that address closure weld conditions and detection reliability for both circumferential and axial cracking in CSS and dissimilar metal weld components need to be conducted as well.

7. REFERENCES

[1] Taylor, T.T., “An Evaluation of Manual Ultrasonic Inspection of Cast Stainless Steel Piping.” U.S. Nuclear Regulatory Commission, NUREG/CR-3753, PNL-5070, (1984).

[2] Rao, G.V., D.E. Seeger, Jr., C. DeFlitch, J.A. Hoffman, R.A. Rees and W.R. Junker. (January 2001). Metallurgical Investigation of Cracking in the Reactor vessel Alpha Loop Hot Leg Nozzle to Pipe Weld at the V. C. Summer Nuclear Generating Station. WCAP-15616. Westinghouse Electric Company LLC, Pittsburgh, PA

[3] Poguet, J., J. Marguet, F. Pichonnat, and L. Chupin. “Phased Array Technology: concepts, probes and applications,” Third Int. Conf. on NDE in Relation to Structural Integrity for Nuclear and Pressurized Components, Seville, Spain (2001).

[4] Doctor, S.R., G.J. Schuster, L.D. Reid, T.E. Hall, “Real Time SAFT-UT System Evaluation and Validation.” US Nuclear Regulatory Commission, NUREG/CR-6344, PNNL-10571, (1996).

[5] Hall, T.E., L.D. Reid, S.R. Doctor, “The SAFT-UT Real-Time Inspection System – Operational Principles and Implementation.” US Nuclear Regulatory Commission, NUREG/CR-5075, PNL-6413, (1988).

[6] Diaz, A.A., S.R. Doctor, B.P. Hildebrand, F.A. Simonen, G.J. Schuster, E.S. Andersen, G.P. McDonald, R.D. Hasse, “Evaluation of Ultrasonic Inspection Techniques for Coarse-Grained Materials”, US Nuclear Regulatory Commission, NUREG/CR-6594, PNNL-11171, (1998).

[7] Anderson, M., S. Cumblidge, S. Doctor, “Applying Ultrasonic Phased Array Technology to Examine Austenitic Coarse-Grained Structures for Light Water Reactor Piping”, Third EPRI Phased Array Inspection Seminar, Seattle, WA, (June 2003).

